Electronic structure of single-crystal rocksalt CdO studied by soft x-ray spectroscopies and *ab initio* calculations

L. F. J. Piper,[*] Alex DeMasi, and Kevin E. Smith

Department of Physics, Boston University, 590 Commonwealth Avenue, Boston, Massachusetts 02215, USA

A. Schleife, F. Fuchs, and F. Bechstedt

Institut für Festkörpertheorie und -optik Friedrich-Schiller-Universität Jena, Max-Wien-Platz 1, D-07743 Jena, Germany

J. Zuniga-Pérez[†] and V. Munoz-Sanjosé

Departamento de Física Aplicada y Electromagnetismo, Universitat de València, C/Dr. Moliner 50, 46100 Burjassot, Spain

Soft x-ray emission spectroscopy (XES) and x-ray absorption spectroscopy (XAS) are employed to investigate the occupied and unoccupied electronic structures in rocksalt-phase single-crystal CdO. Resonant XES at the O K edge reveals a clear Cd $4d$–O $2p$ hybridized peak and momentum-dependent coherent contributions to the resonant emission spectra. Good agreement is obtained between the above-threshold XES and XAS spectra, and the calculated O $2p$ local partial density of states (PDOS). Calculation of the O $2p$ PDOS was performed within the GW framework of many-body perturbation theory.

PACS number(s): 71.55.Gs, 78.70.En, 78.70.Dm, 71.15.Mb

I. INTRODUCTION

Wide band gap oxide semiconductor alloys have become increasingly technologically important, with interest in materials such as $Cd_yMg_xZn_{1-x-y}O$ alloys being motivated for potential applications in optoelectronic devices operating in the ultraviolet and visible region.[1–3] As a result, there is a demand for detailed information on the electronic structure of this class of oxide. We report here an experimental and theoretical study of the electronic structure of CdO, one of the parent oxides in these alloys. Although earlier theoretical studies of rocksalt CdO exist,[4–7] only a few spectroscopic studies exist for direct comparison. These studies employed x-ray photoemission spectroscopy (XPS),[8–10] as well as soft x-ray emission spectroscopy (XES) and x-ray absorption spectroscopy (XAS)[11] to investigate the electronic structure of polycrystalline CdO pellets. Recent improvements in the epitaxial growth of CdO have provided an opportunity to investigate the electronic properties of high-quality crystal thin film rocksalt CdO.[12,13]

We have used synchrotron radiation-excited XES and XAS at the O K edge to measure the valence and conduction band O $2p$ partial densities of states (PDOSs) in single-crystalline CdO. These techniques have previously been used successfully to determine the influence of shallow core-level electrons on the valence band electronic structure in powdered samples of post-transition metal oxides (including CdO).[11] We go beyond these earlier studies not just by examining the single-crystal samples but also by reporting resonant x-ray emission spectroscopy (RXES) spectral changes as a function of excitation energy. For weakly correlated semiconductors, changes in the resonant XES spectra are due to **k** selectivity in the emission process.[14] In recent years, RXES has successfully been developed as a technique for studying the band structure of selected solids.[15] As a "photon-in, photon-out" technique, RXES is insensitive to the degree of sample electrical conductivity, making it an ideal probe of band structure in ionic semiconductors.[16] We find evidence of resonant XES spectral changes in single-crystal CdO due to **k** selectivity, and interpret our results in the context of state-of-the-art valence and conduction band structure calculations which accurately take into account the role of the shallow Cd $4d$ electrons.[7]

II. EXPERIMENTAL AND THEORETICAL METHODS

Single-crystalline CdO(001) films were grown on *r*-plane sapphire ($\bar{1}102$) by metal-organic vapor phase epitaxy. The films were 440 nm thick and had a surface area of 5 mm². Details of the growth and characterization of the samples are reported elsewhere.[13] Single-field Hall measurements of similar samples revealed a degenerate electron concentration of approximately $n=8\times10^{19}$ cm⁻³ with a mobility $\mu=75$ cm² V⁻¹ s⁻¹. The samples were ultrasonically cleaned in acetone, then transferred into the ultrahigh vacuum (UHV) spectrometer chamber (base pressure of $<1\times10^{-10}$ torr). The samples were then annealed at temperatures $<300\ °$C in UHV. The experiments were performed at the undulator beamline X1B at the National Synchrotron Light Source at Brookhaven National Laboratory. This beamline is equipped with a spherical grating monochromator. The absorption spectra were recorded in the total electron yield (TEY) mode by measuring the sample drain current. During the XAS measurements, the entrance and exit slits of the monchromator were set to a width of 20 μm, corresponding to an energy resolution of approximately 0.20 eV for an incident photon energy of 530 eV (the O K-edge region). A gold mesh was used to measure the incident beam intensity and subtract any variations in sample drain current related to the optics rather than the sample electronic structure. The photon energy was calibrated to the O K edge and Ti L edge from rutile TiO₂ measured during the experiment.[17] The emission spectra were recorded using a Nordgren-type grating spectrometer.[18]

A 5 m 1200 line/mm grating was used in first order of diffraction set to an energy resolution of 0.37 eV at the O K edge, with an acquisition time of up to 60 min per emission spectrum. The emission energy axis was calibrated to second order L edge of Zn.[19] Note that the minimal sample surface processing undertaken here is quite adequate for XES measurements given that the sampling depth of the spectroscopy is approximately 100 nm. XAS spectra recorded in a TEY mode are more surface sensitive, but our earlier study of CdO powder pellets revealed no significant difference between XAS spectra recorded in the TEY mode and those recorded in the more bulk-sensitive total fluorescent yield mode.[11] Thus, we consider the XAS spectra recorded in a TEY mode suitable for investigating the unoccupied bulk states of the present CdO thin films without extensive surface preparation.

Theoretical calculations of the PDOS for rocksalt CdO were performed to compare to the XES and XAS spectra. Since the final state in the x-ray emission process contains a hole in the valence band rather than the core level, the soft x-ray emission spectra reflect the ground state PDOS provided that the final state rule is valid. To be fully rigorous, XAS spectra should be compared to calculations which take into account core-hole effects, but these effects are neglected here. The calculations were performed within the framework of hybrid density functional theory (DFT) using the recently proposed HSE03 functional for exchange and correlation.[20] Quasiparticle effects were taken into account by a subsequent GW correction of the HSE03 eigenvalues using many-body perturbation theory. In the GW calculations, the Coulomb potential was fully screened using the random-phase approximation dielectric function based on the HSE03 eigenvalues and functions.[21] These calculations go beyond those reported previously by Schleife *et al.* for rocksalt CdO,[7] where electronic excitation energies have been calculated without taking into account the reaction of the electronic system to the presence of an additional electron (XAS) or hole (XES). Recently, it has been shown that the combination of DFT+HSE03 and GW calculations gives excellent values for the fundamental gaps and d-band positions of many semiconductors.[22] It is well known that the inclusion of quasiparticle corrections opens the gap and increases the electron binding energies. However, the conventional perturbation theory treatment of the GW corrections on top of eigenfunctions from a DFT starting point with a local or semilocal exchange-correlation functional does not reproduce experimental values for compounds of first-row elements. In contrast, the DFT results obtained with a nonlocal exchange-correlation potential are much closer to the final quasiparticle energies. Consequently, we consider the perturbative treatment of GW corrections computed with the HSE03 electronic structure to be much more reliable.

III. RESULTS

Figure 1(a) presents the O K-edge XES spectrum recorded with an incident energy of $h\nu = 554.2$ eV (above threshold) and the sample normal set 50° to the optical axis of the spectrometer, while Fig. 1(b) presents the XAS spectrum re-
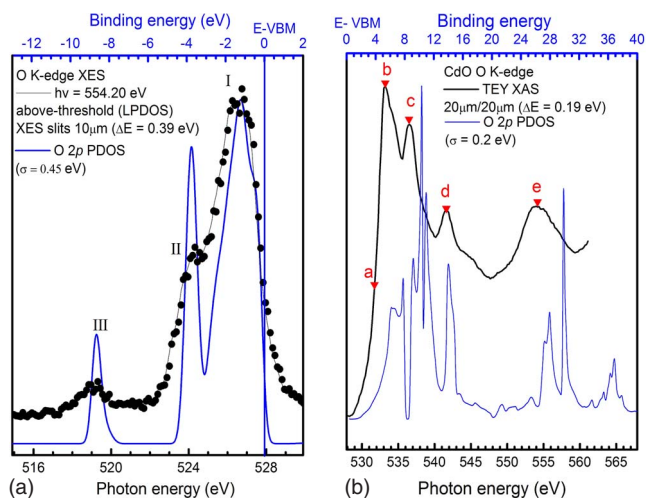

FIG. 1. (Color online) The O k-edge (a) XES and (b) XAS spectra of rocksalt CdO. The XES spectrum includes a three-point adjacent average smoothing (thin black line) as a guide for the eyes. The (a) occupied and (b) unoccupied HSE03+GW calculated O $2p$ PDOS (with a Gaussian broadening) are plotted below the respective spectra for direct comparison. The incident energies used to excite the resonant emission spectra in Fig. 2 are indicated with triangles on the XAS spectrum.

corded at an angle of 50° between the incident photon beam and the surface normal. The XES spectrum displays three peaks identified by numerals I, II, and III. Peaks I and II correspond to the predominantly O $2p$ derived valence band states. Peak III at ~519 eV is associated with transitions into the O $1s$ core hole from electrons in O $2p$ states hybridized with Cd $4d$ shallow electrons, in agreement with early XES studies of polycrystalline binary post-transition oxides.[11] The separation between peaks I and III of ~8.1 eV is consistent with the value of 8.7 eV reported in a recent XPS study of rocksalt CdO single crystals for the separation of the Cd $4d$ shallow core level to the lowest binding energy valence band feature.[23] The O K-edge XAS spectrum displays a similar spectral shape as from CdO pellets.[11]

Figures 1(a) and 1(b) also include the results of our calculation of the occupied O $2p$ PDOS which has been broadened by a Gaussian of full width at half maximum (FWHM) of 0.45 eV to facilitate comparison with the XES spectrum, while the unoccupied O $2p$ PDOS was broadened with a Gaussian of FWHM=0.2 eV for comparison with the XAS spectrum. The occupied PDOS has been rigidly shifted so that peak I in the XES spectrum and the lowest binding energy peak in the calculation coincide, and the valence band maximum (VBM) (zero binding energy) corresponds to an emission energy of 527.9 eV. This method was favored over an extrapolation of the XES VBM due to the strongly nonlinear form of the O K-edge high emission energy tail. Agreement between the XES peaks II and III, and the calculated PDOS is observed following this energy shift. Our earlier XES spectra from polycrystalline CdO were compared to the results of the Hartree–Fock calculations,[11] rather than DFT that neglected quasiparticle effects.[9] The Hartree–Fock calculations better produced the total density of states for comparisons with the valence band XPS (i.e., the calcula-

tions better reproduced the the Cd $4d$ VBM separation). Here, we find improved agreement between our quasiparticle calculation[22] and XES [Fig. 1(a)] over these earlier Hartree–Fock calculations. This is most notable when comparing the Cd $4d$–O $2d$ hybrid state (i.e., peak III) with earlier studies.[11] Furthermore, our calculations provide us with the unoccupied O $2p$ PDOS. While there is general agreement with our earlier study of CdO pellets in terms of the energy separation between the spectral features,[11] the relative intensity of the lowest energy feature in the XAS spectra differs. We consider that our crystalline samples are likely to give sharper XAS features than those observed for polycrystalline samples, in particular, for core-exciton features. This may partly explain the discrepancy between the XAS spectrum and theoretical result in Fig. 1(b). We also note that since our calculations included excited-state self-energy corrections, we consider the slight energetic shift of ~1.5 eV between the experimental and theoretical peaks and enhancement of the intensity of the first peak as being due to excitonic effects. Such a shift has been noted for InN recently, where the separation was considered to give an estimate of the binding energy of the p-like conduction band N $1s$ core-hole exciton.[24] Likewise, the shift between experiment and theory in Fig. 1(b) may provide an estimate of the p-like conduction band O $1s$ core-hole exciton.

For weakly correlated systems, such as semiconductors, resonant x-ray emission spectra consist of an incoherent local PDOS contribution and a **k**-selective coherent contribution.[15] In order to distinguish between these contributions, the PDOS fraction (i.e., an XES spectrum recorded well above threshold) is often subtracted from raw resonant XES spectra.[15,16,24] We recorded O K-edge XES spectra using a range of excitation energies, marked on the XAS spectrum in Fig. 1(b). We then subtracted the above-threshold XES spectrum from each of these recorded XES spectra, while ensuring that the difference spectra did not display negative intensity. The resulting coherent **k**-selective emission spectra of the valence band region, normalized to their maxima, are presented in Fig. 2. We find two distinct spectral changes as the excitation energy is increased through the O K absorption edge: (i) an increase in the relative height of peak at ~524 eV and (ii) the splitting of a single peak at 526.8 eV into two peaks at 525.5 and 527.2 eV. Due to absorption and emission being coupled in a fast coherent scattering process, direct comparisons can be made between the resonant emission spectra and the calculated valence bands around certain high symmetry points. Comparisons of the RXES spectra with the theoretical computations allow us to explain the PDOS shifts in terms of the valence band dispersion of bands with predominantly O $2p$-like character.

Figure 3 plots the bulk Brillouin zone band dispersion obtained from the hybrid DFT computations. The relative strength of O $2p$-like orbital character of each band is indicated by the length of the vertical error bars. Also plotted alongside is the resultant O $2p$ PDOS, with the relative positions of the excitation energies used in Fig. 2 marked by the corresponding label. From direct comparison between the band structure and resultant PDOS, the regions in the BZ excited by the incident excitation energy are as follows: (a) $h\nu$=531.8 eV, close the Γ point; (b) $h\nu$=533.2 eV, near the
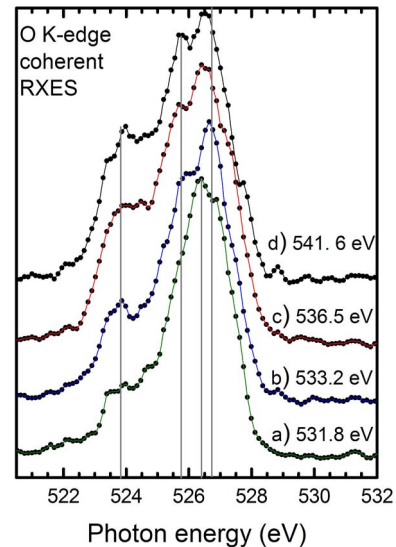

FIG. 2. (Color online) The coherent **k**-selective contribution of the resonant XES spectra, normalized to their maxima and vertically offset.

L point and the W-K region; for the higher energies (c) $h\nu$=536.5 eV and (d) $h\nu$=541.6 eV, the X-W-K region is predominantly excited; these are marked on the band structure plot of Fig. 3

In spectrum (a) in Fig. 2, we begin with a spectrum almost entirely dominated by the peak at 526.8 eV and a small shoulder at 524 eV due to strong coherent contributions from near the Γ point (where the bands are dispersing toward each other). By increasing the excitation energy to $h\nu$=533.2 eV, coherent emission originates from both near the L point and W-K region. This results in two distinct peaks either side of the 526.8 eV; the first at 527.2 eV is from the L point valence band, while the second at 525.5 eV is from the valence bands in the W-K region. By inspecting spectra (c) and (d), we notice only slight changes compared to spectrum (b) in
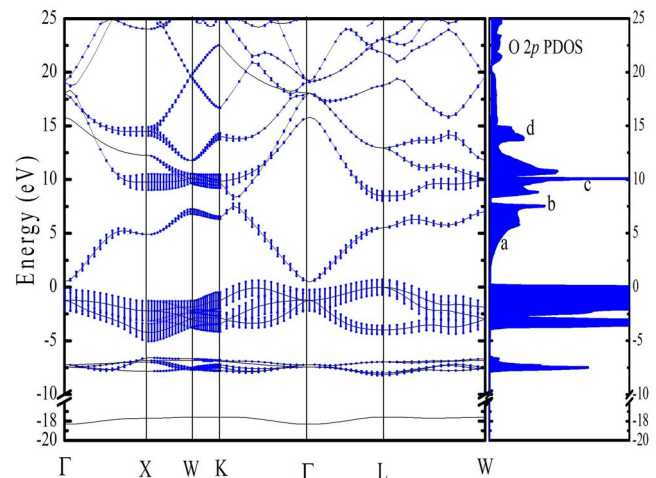

FIG. 3. (Color online) The HSE03 calculated band structure and O $2p$ partial density of states for rocksalt CdO. Labels (a)–(d) refer to incident resonant excitation energies used to excite the x-ray emission process (see text for details).

Fig. 2. This can be considered as the coherent emission being due to coherent contributions dominating from the *X-W-K* regions for these higher energies.

IV. CONCLUSION

We have presented an experimental and theoretical study of the valence and conduction band O 2*p* densities of states of rocksalt CdO using soft x-ray emission and absorption spectroscopies and *ab initio* band structure calculations taking into account many-body effects. Excellent agreement between the XES and XAS spectra, and the calculations is reported. Pronounced changes in the coherent contributions of the resonant XES spectra are identified as being due to **k** selectivity in the resonant x-ray emission process, and their dispersions are supported by our band structure calculations.

*lfjpiper@physics.org

[†]Present address: Centre de Recherche sur l'Hétéro-Epitaxie et ses Applications (CRHEA), Centre National de la Recherche Scientifique (CNRS), Rue Bernard Gregory, 06560 Valbonne, France.

[1] A. Ohtomo, M. Kawasaki, T. Koida, H. Koinuma, Y. Sakurai, Y. Yoshida, M. Sumiya, S. Fuke, T. Yasuda, and Y. Segawa, Mater. Sci. Forum **264**, 1463 (1998).

[2] A. Ohtomo, M. Kawasaki, T. Koida, K. Masubuchi, H. Koinuma, Y. Sakurai, Y. Yoshida, T. Yasuda, and Y. Segawa, Appl. Phys. Lett. **72**, 2466 (1998).

[3] A. Ohtomo, S. Takagi, K. Tamura, T. Makino, Y. Segawa, H. Koinuma, and M. Kawasaki, Jpn. J. Appl. Phys., Part 2 **45**, L694 (2006).

[4] J. E. Jaffe, R. Pandey, and A. B. Kunz, Phys. Rev. B **43**, 14030 (1991).

[5] E. Menendez-Proupin, G. Gutierrez, E. Palmero, and J. L. Pena, Phys. Rev. B **70**, 035112 (2004).

[6] A. Janotti, D. Segev, and C. G. Van de Walle, Phys. Rev. B **74**, 045202 (2006).

[7] A. Schleife, F. Fuchs, J. Furthmüller, and F. Bechstedt, Phys. Rev. B **73**, 245212 (2006).

[8] Y. Dou, T. Fishlock, R. G. Egdell, D. S. L. Law, and G. Beamson, Phys. Rev. B **55**, R13381 (1997).

[9] Y. Dou, R. G. Egdell, D. S. L. Law, N. Harrison, and B. G. Searle, J. Phys.: Condens. Matter **10**, 8447 (1998).

[10] Y. Dou, R. G. Egdell, T. Walker, D. S. L. Law, and G. Beamson, Surf. Sci. **398**, 199 (1998).

[11] C. McGuinness, C. Stagarescu, P. Ryan, J. Downes, D. Fu, K. Smith, and R. Egdell, Phys. Rev. B **68**, 165104 (2003).

[12] A. B. M. A. Ashrafi, H. Kumano, I. Suemune, Y. W. Ok, and T. Y. Seong, Appl. Phys. Lett. **79**, 470 (2001).

[13] J. Zuniga-Perez, C. Munuera, C. Ocal, and V. Munoz-Sanjose, J. Cryst. Growth **271**, 223 (2004), and references therein.

[14] A. Kotani and S. Shin, Rev. Mod. Phys. **73**, 203 (2001).

[15] S. Eisbitt and W. Eberhardt, J. Electron Spectrosc. Relat. Phenom. **110-111**, 335 (2000).

[16] V. N. Strocov, T. Schmitt, J. E. Rubensson, P. Blaha, T. Paskova, and P. O. Nilsson, Phys. Rev. B **72**, 085221 (2005).

[17] R. Ruus, A. Kikas, A. Saar, A. Ausmees, E. Nommiste, J. Aarik, A. Aidla, T. Uustare, and I. Martinson, Solid State Commun. **104**, 199 (1997).

[18] J. Nordgren, G. Bray, S. Cramm, R. Nyholm, J. E. Rubensson, and N. Wasadahl, Rev. Sci. Instrum. **60**, 1690 (1989).

[19] *Center for X-Ray Optics and Advanced Light Source X-Ray Data Handbook*, 2nd ed., edited by A. Thompson and D. Vaughan, (Berkeley, California, 2001), http://xdb.lbl.gov/

[20] J. Heyd, G. E. Scuseria, and M. Ernzerhof, J. Chem. Phys. **118**, 8207 (2003).

[21] M. Shishkin and G. Kresse, Phys. Rev. B **74**, 035101 (2006).

[22] F. Fuchs, J. Furthmüller, F. Bechstedt, M. Shishkin, and G. Kresse, Phys. Rev. B **76**, 115109 (2007).

[23] L. F. J. Piper, P. H. Jefferson, T. D. Veal, C. F. McConville, J. Zuniga-Pérez, and V. Munoz-Sanjosé, Superlattices Microstruct. **42**, 197 (2007).

[24] L. F. J. Piper, L. Colakerol, T. Learmonth, P.-A. Glans, K. E. Smith, F. Fuchs, J. Furthmüller, F. Bechstedt, Y. C. Chen, T. D. Moustakas *et al.*, Phys. Rev. B **76**, 245204 (2007).